Earthquakes and Structures, *Vol. 18, No. 4 (2020) 437-449*
DOI: https://doi.org/10.12989/eas.2020.18.4.437

Influence of infill walls on modal expansion of distribution of effective earthquake forces in RC frame structures

Taner Ucar*

Department of Architecture, Dokuz Eylul University, 35390, Buca, Izmir, Turkey

(*Received June 19, 2019, Revised January 14, 2020, Accepted February 26, 2020*)

Abstract. It is quite apparent that engineering concerns related to the influence of masonry infills on seismic behavior of reinforced concrete (RC) structures is likely to remain relevant in the long term, as infill walls maintain their functionalities in construction practice. Within this framework, the present paper mainly deals with the issue in terms of modal expansion of effective earthquake forces and the resultant modal responses. An adequate determination of spatial distribution of effective earthquake forces over the height of the building is highly essential for both seismic analysis and design. The possible influence of infill walls is investigated by means of modal analyses of two-, three-, and four-bay RC frames with a number of stories ranging from 3 to 8. Both uniformly and non-uniformly infilled frames are considered in numerical analyses, where infill walls are simulated by adopting the model of equivalent compression strut. Consequently, spatial distribution of effective earthquake forces, modal static base shear force response of frames, modal responses of story shears from external excitation vector and lateral floor displacements are obtained. It is found that, infill walls and their arrangement over the height of the frame structure affect the spatial distribution of modal inertia forces, as well as the considered response quantities. Moreover, the amount of influence varies in stories, but is not very dependent to bay number of frames.

Keywords: infilled RC frames; equivalent compression strut; modal analysis; modal expansion; effective earthquake forces

1. Introduction

Reinforced concrete structures commonly infilled with unreinforced clay brick masonry infill walls comprise the significant portion of the entire building stock all over the world. Although recognizing their influence on overall seismic response of structures, infill walls are generally not taken into account during seismic design due to some uncertainties related to modelling issues and considered in principle as non-structural elements. However, some contemporary seismic codes (e.g., EC8 (2004)) and standards (e.g., FEMA 356 (2000), ASCE/SEI 41-06 (2007), ASCE/SEI 41-13 (2014)) include special provisions related to infill walls, where procedures for determination of engineering properties of masonry infills are introduced and masonry infill panels are considered in the analytical model. Consequently, the engineering application in this manner causes infilled frames to remain a controversial topic in scientific literature. It is quite apparent that infill walls will maintain their architectural, functional and aesthetic efficiencies both in current and future construction practices. Accordingly, extensive efforts towards investigating and evaluating the seismic response of infilled RC frame structures still present a relevant challenge.

The variations in elastic and inelastic seismic response of frame structures due to infill walls and the influence of masonry infills on seismic performance of RC frames subjected to earthquake ground motions have been a subject to many numerical and experimental studies (Lu 2002, Canbay *et al*. 2003, Decanini *et al*. 2004, Su *et al*. 2005, Kurt *et al*. 2011, Ricci *et al*. 2011, Chrysostomou and Asteris 2012, Fiore *et al*. 2012, Hak *et al*. 2012, Manfredi *et al*. 2012, Manos *et al*. 2012, Uva *et al*. 2012, Celarec and Dolsek 2013, Šipoš *et al*. 2013, Lima *et al*. 2014, Lucchini *et al*. 2014, Morandi *et al*. 2014, Cavaleri and Di Trapani 2015, Jiang *et al*. 2015, Emamia and Mohammadi 2016, Fenerci *et al*. 2016, Sassun *et al*. 2016, Zhai *et al*. 2016, Muthukumar *et al*. 2017, Zhang *et al*. 2017, Furtado *et al*. 2018, Repapis and Zeris 2019). In numerical works, the behavior of infill walls has been simulated through so-called micro- and macro-modelling techniques and both of them have been widely accepted by engineering communities as reasonably accurate numerical modelling techniques of infill walls (Asteris 2008, Dolsek and Fajfar 2008, Rodrigues *et al*. 2010, Stavridis and Shing 2010, Kakaletsis *et al*. 2011, Karayannis *et al*. 2011, Celarec *et al*. 2012, Uva *et al*. 2012, Favvata *et al*. 2013, Haldar *et al*. 2013, Cavaleri and Di Trapani 2014, Campione *et al*. 2015, Furtado *et al*. 2015, Mazza 2015, Redmond *et al*. 2016, De Risi *et al*. 2017, Yekrangnia and Mohammadi 2017, Blasi *et al*. 2018, De Domenico *et al*. 2018, Šipoša *et al*. 2018, Tabeshpour and Arasteh 2019). On the other hand, the out-of-plane behavior of masonry infill walls has also been studied extensively in the recent years (Tu *et al*. 2010, Varela-Rivera *et al*. 2011, Manfredi and Masi 2014, Akhoundi *et al*. 2015, Furtado *et al*. 2016, Asteris *et al*. 2017, Onat *et al*. 2018).

*Corresponding author, Associate Professor
E-mail: taner.ucar@deu.edu.tr

http://www.techno-press.org/?journal=eas&subpage=7
ISSN: 2092-7614 (Print), 2092-7622 (Online)

A literature survey indicates that infill walls increase the lateral stiffness of frames, lead to a shortening in periods of vibration, and thereby induce a notable change both in seismic demand and structural capacity, in terms of dynamic analysis. However, shortening in period of vibration is not alone responsible for such change on earthquake response of a structure. The earthquake response of an elastic multi-degree-of-freedom (MDOF) structure is the product of modal static response of MDOF system subjected to inertia forces associated with natural modes of vibration and dynamic response of nth mode linear single-degree-of-freedom (SDOF) system excited by earthquake ground motion. Consequently, it is quite important to recognize the possible influence of infill walls on spatial distribution of effective earthquake forces over the height of the structure, which has not been specifically taken into consideration in previous works.

The main objective of the current study is to investigate the effect of infill walls on modal expansion of spatial distribution of effective earthquake forces in RC frame structures. Hence, starting from dynamics of MDOF systems, modal expansion of earthquake excitation vector, as well as modal response quantities in terms of lateral forces and displacements, are first obtained, and followed by introducing the influence of infill walls on spatial distribution of effective earthquake forces. The numerical part of the study consists of modal analyses of several, both bare and infilled, RC frames with different number of stories and bays, where uniformly infilled and soft story frames have been taken into account. Spatial distribution of modal inertia forces, normalized base shear forces associated with first few modes of vibration, distribution of story shears over the height of frames, and finally lateral floor displacements for the fundamental mode are obtained. The results are discussed in detail and compared within the frame of above stated concerns.

2. Modal expansion of effective earthquake forces

The compact matrix form of governing differential equations of motion of an MDOF building subjected to horizontal earthquake ground motion excitation is as follows

$$m\ddot{u} + c\dot{u} + ku = -ml\ddot{u}_g(t) \equiv F_{eff}(t) \tag{1}$$

where $u(t)$ is the vectorial displacement variable composed of N lateral story displacements relative to the ground, m, c and k are the mass, damping and lateral stiffness matrices of an MDOF system. l is the influence vector of order N transmitting the ground displacement $u_g(t)$ to the dynamic DOF's as a result of rigid body motion of the base and for shear frames, its each element is equal to unity, i.e. l=1. The right-hand side of Eq. (1) can be considered as effective earthquake forces.

The spatial distribution of effective earthquake forces over the height of the structure is defined by the vector s, which is independent of the time variation of effective earthquake forces. The vector s can be expanded as a summation of modal inertial forces developed on the masses. Accordingly, the expansion vector of inertial forces associated with natural vibration modes becomes (Chopra 2012)

$$s = m1 = \sum_{n=1}^{N} s_n = \sum_{n=1}^{N} \Gamma_n m\phi_n \tag{2}$$

where s_n is the contribution of the nth mode to the excitation vector s and its independent of how the modal vector ϕ_n is normalized. The coefficient Γ_n can be easily derived by substituting the displacement vector expressed as a linear combination of the orthogonal modal vectors in Eq. (1) and pre-multiplying by ϕ_n^T:

$$\Gamma_n = \frac{\phi_n^T m1}{\phi_n^T m\phi_n} = \frac{L_n}{M_n} \tag{3}$$

In Eq. (3), M_n is the modal mass and L_n is the modal excitation factor.

The effective earthquake forces can then be expressed as

$$F_{eff}(t) = \sum_{n=1}^{N} F_{eff,n}(t) = \sum_{n=1}^{N} -s_n\ddot{u}_g(t) \tag{4}$$

where $\ddot{u}_g(t)$ defines the time variation of effective forces.

The static floor displacements due to modal inertia forces s_n can be obtained as

$$u_n^{st} = k^{-1}s_n = \frac{\Gamma_n}{\omega_n^2}\phi_n \tag{5}$$

Eqs. (4) and (5) clearly indicate that the response of an MDOF system to earthquake induced ground motion is completely in the nth mode. Accordingly, it is quite apparent that the influence of infill walls on natural vibration modes of an MDOF structure will result in different spatial distribution of effective earthquake forces. Infill walls are expected to affect the response of an MDOF system to $F_{eff}(t)$ by acting on free vibration characteristics of the system.

Recognizing the influence of infill walls on s_n and u_n^{st} vectors, will result in considering the infill walls and their possible effects on seismic analysis and design of RC structures, since the earthquake response of the structure can be directly obtained as the product of modal static responses of MDOF system to external forces s_n and response history analysis of the n*th* mode SDOF system excited by earthquake ground motion. Accordingly, the lateral forces $f_n(t)$ at the floor levels can be expressed as

$$f_n(t) = s_n A_n(t) \tag{6}$$

where $A_n(t)$ is the pseudo-acceleration response of the nth mode SDOF system under earthquake ground motion, i.e. pseudo acceleration. Similarly, the lateral displacement vector of a structure excited by earthquake ground motion can be formulated as follows

$$u_n(t) = u_n^{st}A_n(t) = \frac{\Gamma_n}{\omega_n^2}\phi_n A_n(t) \tag{7}$$

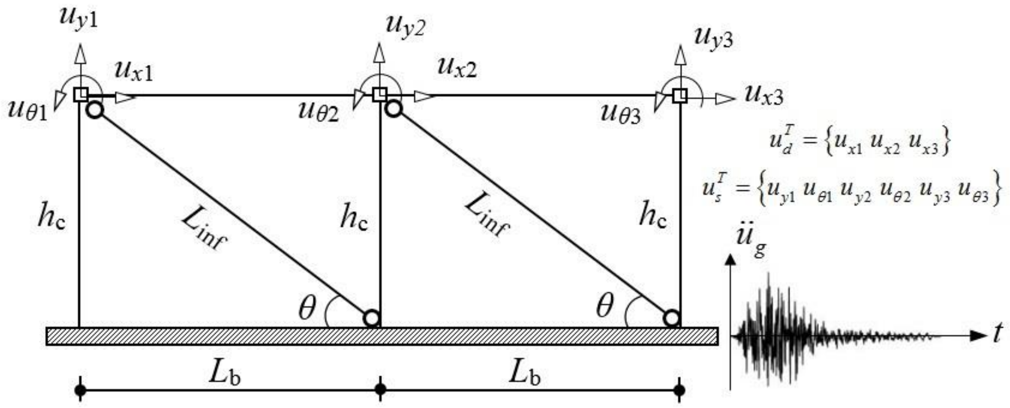

Fig. 1 Analytical model of a single story two-bay infilled frame

In implementation of modal response spectrum analysis in the seismic design of RC buildings, $A_n(t)_{\max}$ can be readily obtained as the ordinate of the elastic design spectrum, i.e. the peak value of total acceleration. It should be noted that infill walls could also have an effect on spectral ordinate of design acceleration spectrum by shortening the natural period of the structure.

3. Influence of infill walls

The influence of infill walls on modal expansion of spatial distribution of effective earthquake forces can be taken into consideration by starting from the derivation of stiffness matrix of the system. Infill walls are simulated by adopting the model of equivalent compression strut referred to as the most simplified yet reasonably accurate macro-model. In this model the elastic in-plane stiffness of masonry infill panel prior to cracking is represented by an equivalent diagonal compression strut. Accordingly, a diagonal pin jointed strut having the same thickness and modulus of elasticity as the infill panel it represents is connected between the beam-column joints (Fig. 1). Also, in accordance with FEMA 356 (2000), the width of the equivalent diagonal compression strut (a) is calculated as follows

$$a = 0.175\left(\lambda_1 h_c\right)^{-0.4} L_{\text{inf}} \tag{8}$$

Where

$$\lambda_1 = \sqrt[4]{\frac{E_{\text{me}} t_{\text{inf}} \sin 2\theta}{4 E_{\text{fe}} I_c h_{\text{inf}}}} \tag{9}$$

In Eqs. (8) and (9), h_c is column height between centerlines of beams, h_{inf} is height of infill panel, E_{fe} is expected modulus of elasticity of frame material, E_{me} is expected modulus of elasticity of infill material, I_c is moment of inertia of column, L_{inf} is diagonal length of infill panel, t_{inf} is thickness of infill panel, as well as of equivalent strut, respectively.

The stiffness matrix of the above single story two-bay infilled frame is developed by employing the direct stiffness method based on the definition of stiffness influence coefficients. Ignoring the axial deformations of beams and columns significantly reduces the degrees of freedom (DOFs) of the system. With this assumption, the DOFs of a planar shear frame are the rotational DOFs of nodes and the translational DOFs of the stories. By imposing translational and rotational unit displacements respectively in the direction of DOFs, the partitioned stiffness matrix form of the considered frame is obtained as

$$k = \begin{bmatrix} k_{dd} & k_{ds} \\ k_{sd} & k_{ss} \end{bmatrix} \tag{10}$$

The corresponding stiffness coefficients of Eq. (10) are expressed as below

$$k_{dd} = \left\{ \frac{36EI_c}{h_c^3} + \frac{2EA}{L_{\text{inf}}} \cos^2\theta \right\} \tag{11a}$$

$$k_{ds} = \left\{ \frac{6EI_c}{h_c^2} \quad \frac{6EI_c}{h_c^2} \quad \frac{6EI_c}{h_c^2} \right\} \tag{11b}$$

$$k_{ss} = \begin{bmatrix} \frac{4EI_c}{h_c} + \frac{4EI_b}{L_b} & \frac{2EI_b}{L_b} & 0 \\ \frac{2EI_b}{L_b} & \frac{4EI_c}{h_c} + \frac{8EI_b}{L_b} & \frac{2EI_b}{L_b} \\ 0 & \frac{2EI_b}{L_b} & \frac{4EI_c}{h_c} + \frac{4EI_b}{L_b} \end{bmatrix} \tag{11c}$$

and $k_{sd} = \{k_{ds}\}^T$.

It should be noted that the contribution of infill walls is incorporated into k_{dd} matrix. Since earthquake forces act on the dynamic DOFs (u_d), the static DOFs (u_s) can be eliminated during modal response history analysis by the method of static condensation. Accordingly, the condensed stiffness matrix (k_d) with order of the number of dynamic DOFs is given by

$$k_d = k_{dd} - k_{ds} k_{ss}^{-1} k_{sd} \tag{12}$$

The analysis procedure applied in the study is shown schematically in Fig. 2

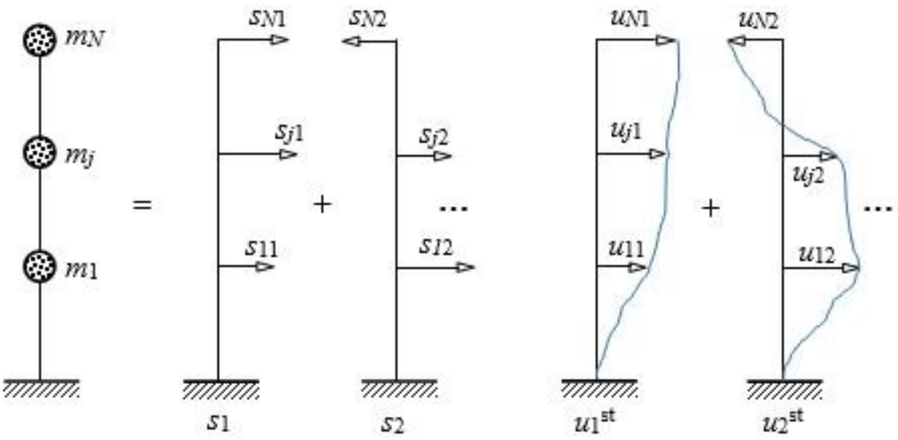

Fig. 2 Conceptual characterization of modal expansion of forces and displacements

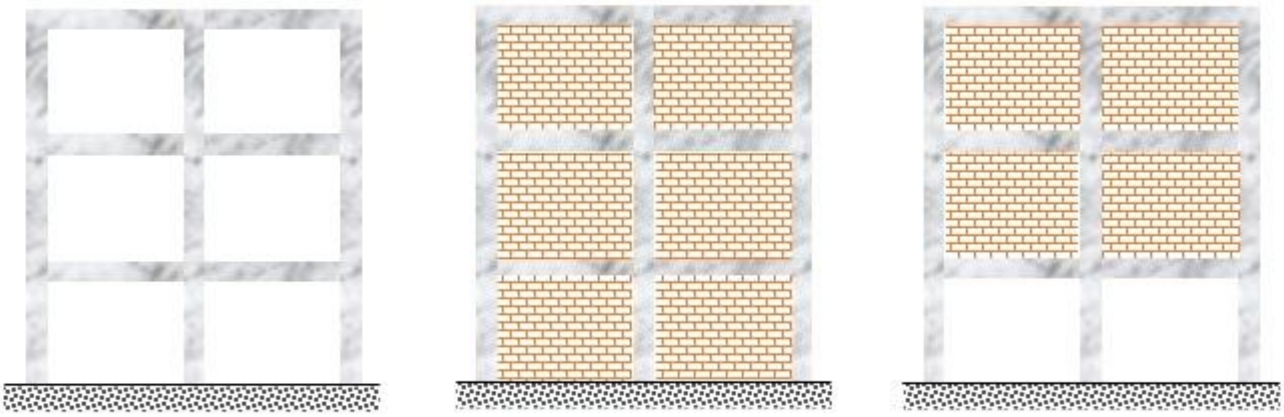

(a) Bare frame (b) Uniformly infilled frame (c) Soft story frame

Fig. 3 Typical view of frame models

4. Application of numerical studies

4.1 Description of frames

The numerical part of the study is composed of modal analyses of two-, three-, and four-bay RC frames with a number of stories ranging from 3 to 8. The length of all spans is assumed to be identical and taken as 5 m, a commonly encountered value in RC building construction practice. The typical story height is 2.7 m. In order to examine the possible effects of infill walls on modal expansion of spatial distribution of effective earthquake forces in RC frame structures, three groups of frames as bare, uniformly infilled and soft story are generated. Accordingly, a total of 54 RC frames are analyzed in the study. Typical view of two-bay bare, uniformly infilled and soft story frames is presented in Fig. 3.

The selected frames are 2D models of an external frame of a 3D structure and the magnitudes of gravity loads are determined accordingly. Live load participation factor is taken as 0.30 and story weights, as well as the related seismic masses, are determined as the combination of dead loads and 30% of live loads. Accordingly, the lumped seismic floor masses are calculated as m_j=36.5 tons, 54 tons and 71 tons, and the seismic masses assigned to top floor are m_N=27.5 tons, 40.5 tons and 53.5 tons, respectively, for two-, three-, and four-bay frames.

The compressive strength of concrete is 30 MPa and the corresponding modulus of elasticity of concrete material, which is frequently related with its compressive strength, is taken to be E_{fe}=32000 MPa. The yield strength of reinforcement steel is assumed to be 420 MPa. The frames are assumed to be located on soil profile type ZD, the counterpart of NEHRP site class D, and assigned to Seismic Design Category 1, e.g. the value of short period design response acceleration S_{DS} is greater than 0.75g. The considered frames are designed under the horizontal elastic design spectrum of Turkish Seismic Design Code (TSDC, 2018) by employing a response reduction factor of R=8. The design spectrum of TSDC (2018) is an elastic response spectrum for 5% equivalent viscous damping used to represent the design basis ground motion. As a result of analyses performed on two-dimensional analytical models of frames created in SAP2000 (2018) platform, rectangular beams of 250 mm width and 500 mm height, and square columns with different dimensions mainly based on story numbers are designed in accordance with TSDC (2018). The column dimensions (h = b) are given in Table 1.

The thickness of infill panels composed of vertically cored brick units and 10 mm thick mortar joints is assumed

Table 1 Some geometrical parameters of equivalent strut analogy

Story Number	$h=b$ (mm)	L_{inf} (m)	θ (°)	a (mm)
3	350	5.256	27.78	605
4	400	5.212	28.04	632
5	450	5.167	28.30	657
6	500	5.124	28.57	679
7	500	5.124	28.57	679
8	550	5.080	28.84	699

to be t_{inf}=200 mm. The expected value of elastic modulus for masonry in compression is determined in accordance with FEMA 356 (2000) as a function of the expected masonry compressive strength (f_{me}). The masonry condition is taken as fair, based on visual observations of the author on the brick masonry construction quality in ordinary residential buildings in Turkey. Accordingly, as specified in FEMA 356 (2000), the corresponding expected masonry compressive strength is calculated as f_{me}=5.38 MPa by multiplying the default lower-bound strength of masonry in fair condition by a factor of 1.3. Consequently, the expected elastic modulus of masonry is found to be E_{me}=2959 MPa.

Masonry infill walls are simulated by equivalent compression struts having the same thickness and modulus of elasticity as the infill panel it represents. The strut is connected between the beam-column joints and moment releases are specified at both ends of the strut in order to prevent the transfer of shear forces and bending moments from frame to infill panel. The width of the equivalent diagonal compression strut (a) calculated in accordance with FEMA 356 (2000) are listed in Table 1 together with some necessary cross sectional and geometrical parameters. The angle θ is equal to the inverse tangent of height-to-length aspect ratio of infill panel.

4.2 Results of analysis and discussion

4.2.1 Spatial distribution of modal inertia forces

In the first phase of the study, free vibration properties of frame structures are computed. Axial deformations of beam and column elements are neglected. Since it is not very practical for hand calculation, the matrix eigenvalue problem of MDOF frames is solved by means of SAP2000 (2018). As a consequence, natural vibration frequencies (ω_n), as well as the corresponding natural periods of vibration (T_n), and natural modes of vibration are determined.

Table 2 presents the calculated results of three natural vibration periods (n=1, 2, 3) of undamped frame systems. As it is expected, the natural periods of vibration of infilled uniformly infilled frames are much shorter than those of bare frames, i.e., the presence of infills increases considerably the lateral stiffness of frames. The natural periods of soft story frames are found to be between the natural periods of bare frames and infilled frames. These results clearly demonstrate that infill walls are expected to affect the seismic response of structures since the pseudo-acceleration response of the nth mode SDOF system under earthquake ground motion is very closely associated to natural vibration period of the structure.

The other issue is that, infill walls and their distribution along the height of the structure are also expected to change the seismic response of the structure by both effecting the natural mode shapes of vibration, i.e. modal vectors, and the natural vibration frequencies. The variation of natural vibration frequencies due to infill walls can be easily evaluated from Table 2. On the other hand, the excitation vector s containing the modal expansion of the spatial distribution of effective earthquake forces is closely dependent to natural mode shapes of vibration. In order to emphasize this point, values of modal property Γ_n are firstly calculated. The natural mode shapes of vibration are normalized with respect to the modal mass, M_n to reduce the amount of arithmetical computations. Accordingly, given in Table 3 are Γ_n values calculated using the mass normalized modal vectors, i.e. M_n=1. Then, s_n vectors, the contribution of the nth mode to the excitation vector s, are computed by means of Eq. (2). Accordingly, the modal expansion of effective earthquake forces associated with a horizontal earthquake ground motion excitation $\ddot{u}_g(t)$ is determined.

Shown in Fig. 4 are the resultant modal inertia force distributions for the fundamental mode of the considered frame structures. In this figure, the scalar components of s_1 vector are normalized with respect to total seismic mass of the structure. The variation in the distribution of effective earthquake forces is particularly dominant in lower stories and they are found to increase when infill walls are considered. When compared to bare frames, the mean increase in effective earthquake forces at the first floor level is 7%, 12.2%, 16.6%, 20%, %21.7 and 23.6%, respectively, for 3 to 8 story frames. The mean increase in effective earthquake forces at the second floor level is calculated to be 1.6%, 4.3%, 7.1%, 9.8%, 11% and 13.1%, respectively, for the same frames. No significant variation in effective earthquake forces due to infill walls is observed in the stories following the second one. Furthermore, they slightly decrease at the top story when compared to those of bare frames.

It becomes more dramatic in the case of soft story frames. The mean increase in effective earthquake forces at the first floor level is found to be 46.5%, 59.6%, 63.2%, respectively, for 3 to 5 story frames. The mean increase is over 60% in other soft story frames. The mean increase in effective earthquake forces at the second floor level of soft story frames is found to be 4.6%, 16.3%, 22.9%, 26.2%, %29.6 and 30.1%, respectively, for 3 to 8 story frames. The increase is not significant at upper floor levels.

It is observed that, the higher mode shapes of vibration do not remain unchanged due to infill walls and their distribution over the height of the structure. However, the expansion vector of inertial forces associated with higher vibration modes does not discussed in detail here since the response of frame structures is mainly controlled by the fundamental mode of vibration. It can be roughly concluded that, infill walls also affect the higher modes of vibration but their contribution to total response is generally small.

Although infill walls affect the spatial distribution of

Table 2 Natural periods of vibration (s)

		Two-bay			Three-bay			Four-bay		
	Mode, N	n=1	n=2	n=3	n=1	n=2	n=3	n=1	n=2	n=3
Bare Frames	3	0.348	0.110	0.064	0.356	0.113	0.066	0.359	0.115	0.068
	4	0.408	0.127	0.069	0.414	0.129	0.071	0.416	0.131	0.072
	5	0.468	0.145	0.077	0.473	0.147	0.079	0.475	0.148	0.080
	6	0.529	0.163	0.086	0.533	0.165	0.088	0.533	0.166	0.089
	7	0.624	0.195	0.105	0.624	0.196	0.106	0.628	0.198	0.108
	8	0.680	0.212	0.113	0.683	0.214	0.116	0.683	0.214	0.116
Infilled Frames	3	0.205	0.071	0.046	0.206	0.071	0.047	0.206	0.071	0.047
	4	0.252	0.084	0.051	0.253	0.085	0.051	0.253	0.085	0.052
	5	0.298	0.098	0.057	0.298	0.098	0.058	0.298	0.098	0.058
	6	0.343	0.112	0.064	0.343	0.112	0.065	0.342	0.112	0.065
	7	0.401	0.131	0.076	0.399	0.131	0.076	0.399	0.131	0.077
	8	0.443	0.144	0.083	0.442	0.145	0.084	0.441	0.144	0.084
Soft Story Frames	3	0.276	0.078	0.047	0.283	0.079	0.048	0.286	0.080	0.048
	4	0.302	0.092	0.053	0.307	0.094	0.054	0.309	0.094	0.054
	5	0.333	0.105	0.060	0.337	0.106	0.060	0.338	0.107	0.061
	6	0.368	0.118	0.067	0.371	0.119	0.067	0.371	0.119	0.068
	7	0.427	0.138	0.079	0.425	0.138	0.079	0.429	0.139	0.080
	8	0.462	0.150	0.085	0.464	0.150	0.086	0.463	0.150	0.086

Table 3 Γ_n values

		Two-bay			Three-bay			Four-bay		
	Mode, N	n=1	n=2	n=3	n=1	n=2	n=3	n=1	n=2	n=3
Bare Frames	3	9.468	-3.003	1.358	-11.534	3.596	-1.588	-13.250	-4.093	1.784
	4	10.837	-3.713	-2.131	13.204	4.476	-2.535	15.166	-5.111	-2.870
	5	-12.029	-4.240	-2.620	-14.656	-5.124	3.140	16.831	-5.859	3.574
	6	13.105	-4.677	-2.975	15.968	-5.657	-3.577	18.333	-6.471	4.078
	7	14.174	-4.998	-3.174	-17.229	-6.061	3.855	19.824	6.927	4.362
	8	15.092	-5.358	3.439	18.385	-6.489	4.146	21.107	-7.427	-4.732
Infilled Frames	3	-9.552	-2.801	1.188	-11.625	-3.376	1.396	-13.347	-3.858	1.575
	4	10.966	-3.498	-1.888	-13.351	4.230	2.248	-15.327	-4.840	-2.553
	5	-12.189	4.028	-2.355	-14.843	4.880	2.825	17.040	-5.587	3.217
	6	13.288	-4.470	2.705	16.182	5.419	-3.256	-18.576	-6.206	3.714
	7	14.356	-4.823	-2.920	17.455	5.859	3.546	-20.065	6.705	4.023
	8	15.290	5.180	3.182	-18.620	-6.287	3.842	21.371	7.203	4.390
Soft Story Frames	3	-9.858	-1.701	0.648	12.008	-1.951	0.714	-13.791	-2.168	0.776
	4	11.310	-2.659	1.252	13.791	3.122	1.427	15.844	-3.513	-1.579
	5	12.506	3.471	1.800	-15.254	4.135	-2.096	17.526	4.688	-2.347
	6	-13.556	4.118	-2.276	-16.531	4.947	2.687	-18.991	5.632	-3.031
	7	-14.631	4.521	-2.505	-17.791	-5.499	3.041	20.492	6.210	-3.361
	8	-15.509	4.994	2.887	18.908	-6.035	3.448	21.715	-6.897	-3.914

modal inertia forces by contributing the elastic stiffness of structures, this variation is not very dependent to bay number of frames. It is observed that, frames with different bays exhibit nearly the same trend in variation of effective earthquake forces.

4.2.2 Normalized base shears

Since it is a very important parameter in seismic analysis and design, the modal static base shear force response of frames to external forces s_n, i.e. the effective modal masses, are also calculated. Base shears are normalized with respect to seismic mass of the structure and the contribution of the first three modes to base shear response is given in Table 4. As expected, the major contribution comes from the fundamental mode in all frames. However, base shear coefficients for the fundamental mode, i.e. base shear to seismic mass ratio, are found to increase due to infill walls. This is a very important finding since the total design lateral force or shear at the base of a structure is distributed over the height of the structure during seismic design. In case of soft story frames, the increase is much higher. It is obvious that, the potential seismic demand in terms of base shears will increase when infill walls are considered in structural analysis. The contribution of the fundamental mode to base shear response is more dominant when infill walls are used as structural elements. Particularly, in case of soft story irregularity, the fundamental mode is much more dominant on seismic response. The nth mode contribution of $V_{bn}^{st}/\Sigma m_j$ to total response is almost independent of bay number of frames.

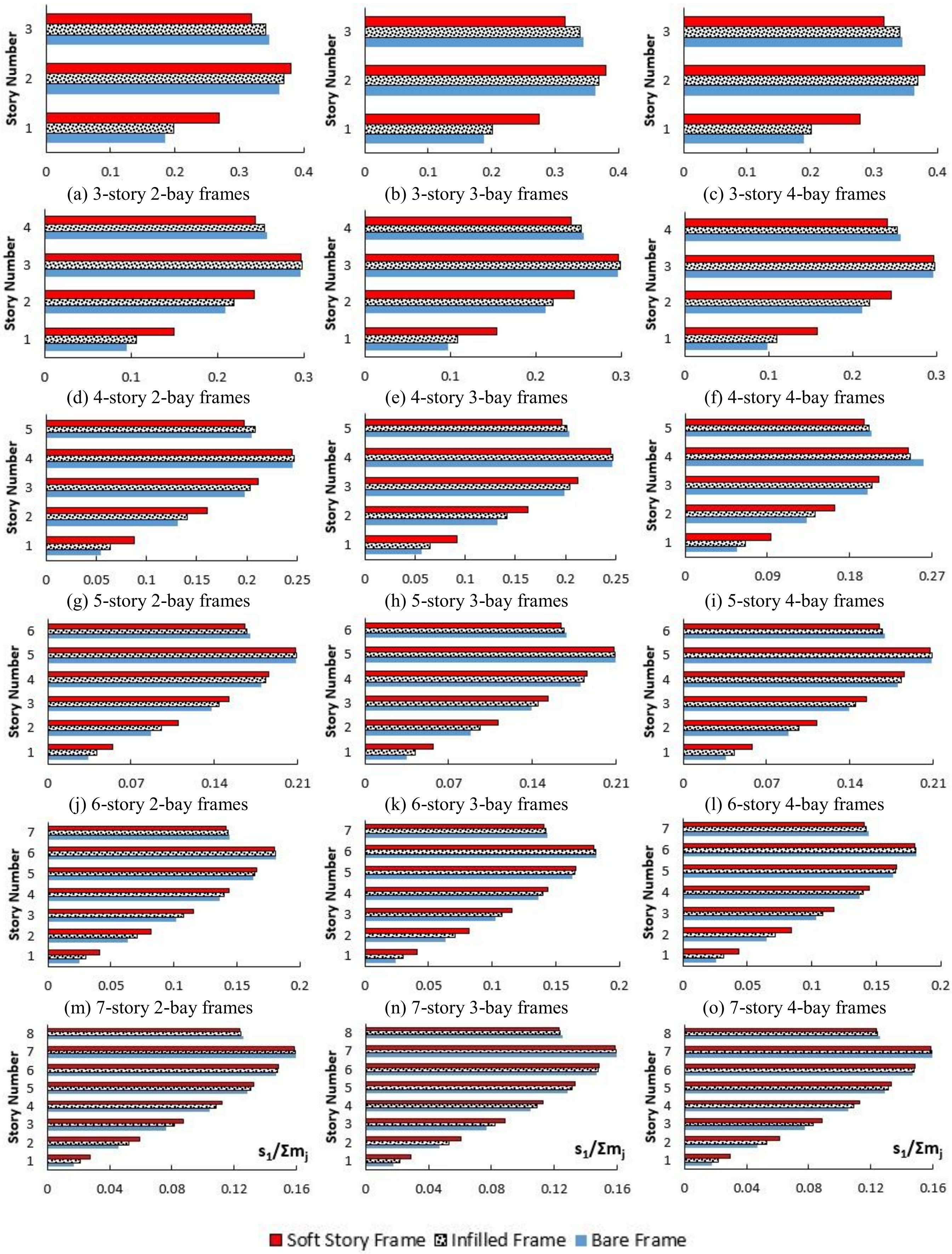

(a) 3-story 2-bay frames (b) 3-story 3-bay frames (c) 3-story 4-bay frames

(d) 4-story 2-bay frames (e) 4-story 3-bay frames (f) 4-story 4-bay frames

(g) 5-story 2-bay frames (h) 5-story 3-bay frames (i) 5-story 4-bay frames

(j) 6-story 2-bay frames (k) 6-story 3-bay frames (l) 6-story 4-bay frames

(m) 7-story 2-bay frames (n) 7-story 3-bay frames (o) 7-story 4-bay frames

(p) 8-story 2-bay frames (q) 8-story 3-bay frames (r) 8-story 4-bay frames

Fig. 4 Modal inertia force distribution for the fundamental mode

Table 4 Mass normalized static base shear forces ($V_{bn}^{st}/\Sigma m_j$)

	Mode, *N*	Two-bay			Three-bay			Four-bay		
		n=1	*n*=2	*n*=3	*n*=1	*n*=2	*n*=3	*n*=1	*n*=2	*n*=3
Bare Frames	3	0.892	0.090	0.018	0.896	0.087	0.017	0.898	0.086	0.016
	4	0.857	0.101	0.033	0.861	0.099	0.032	0.863	0.098	0.031
	5	0.834	0.104	0.040	0.837	0.102	0.038	0.839	0.102	0.038
	6	0.818	0.104	0.042	0.821	0.103	0.041	0.823	0.103	0.041
	7	0.815	0.101	0.041	0.814	0.101	0.041	0.820	0.100	0.040
	8	0.805	0.101	0.042	0.808	0.101	0.041	0.809	0.100	0.041
Infilled Frames	3	0.908	0.078	0.014	0.910	0.077	0.013	0.911	0.076	0.013
	4	0.878	0.089	0.026	0.880	0.088	0.025	0.881	0.088	0.024
	5	0.856	0.094	0.032	0.859	0.093	0.031	0.860	0.092	0.010
	6	0.841	0.095	0.035	0.843	0.095	0.034	0.845	0.094	0.034
	7	0.836	0.094	0.035	0.836	0.094	0.034	0.840	0.094	0.034
	8	0.826	0.095	0.036	0.828	0.094	0.035	0.830	0.094	0.035
Soft Story Frames	3	0.967	0.029	0.004	0.971	0.026	0.003	0.973	0.024	0.003
	4	0.934	0.052	0.011	0.939	0.048	0.010	0.942	0.046	0.009
	5	0.901	0.069	0.019	0.907	0.067	0.017	0.910	0.065	0.016
	6	0.875	0.081	0.025	0.880	0.079	0.023	0.883	0.077	0.022
	7	0.868	0.083	0.025	0.868	0.083	0.025	0.876	0.080	0.024
	8	0.850	0.088	0.029	0.854	0.087	0.028	0.857	0.086	0.028

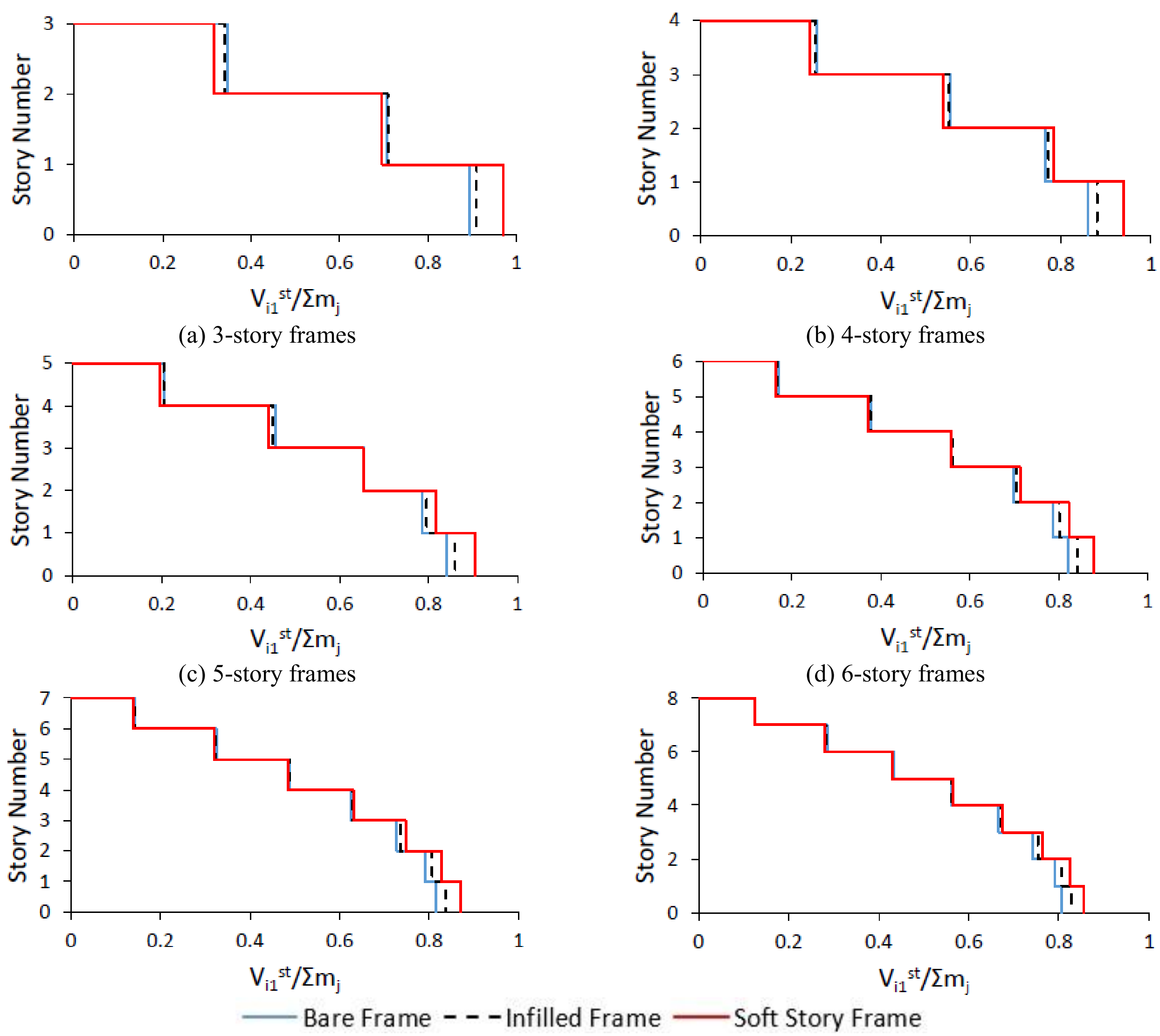

(a) 3-story frames (b) 4-story frames

(c) 5-story frames (d) 6-story frames

(e) 7-story frames (f) 8-story frames

Fig. 5 Mass normalized mean story shears for the fundamental mode

Table 5 The contribution of the fundamental mode to lateral floor displacements relative to the ground ($u_{j1}^{st} \times 10^{-3}$)

Story Number	Displacement Vector	Two-bay			Three-bay			Four-bay		
		Bare	Infilled	Soft Story	Bare	Infilled	Soft Story	Bare	Infilled	Soft Story
3	$u_1^{st} =$ u_{11}^{st}	1.553	0.580	1.424	1.654	0.059	1.533	1.704	0.593	1.589
	u_{21}^{st}	3.063	1.080	2.017	3.213	1.088	2.121	3.282	1.088	2.172
	u_{31}^{st}	3.888	1.329	2.244	4.049	1.334	2.344	4.124	1.332	2.393
4	$u_1^{st} =$ u_{11}^{st}	1.495	0.647	1.293	1.577	0.660	1.383	1.616	0.663	1.431
	u_{21}^{st}	3.308	1.325	2.103	3.437	1.336	2.191	3.490	1.335	2.235
	u_{31}^{st}	4.679	1.806	2.571	4.830	1.814	2.654	4.888	1.810	2.695
	u_{41}^{st}	5.416	2.044	2.801	5.567	2.049	2.880	5.624	2.042	2.919
5	$u_1^{st} =$ u_{11}^{st}	1.441	0.684	1.175	1.510	0.699	1.248	1.540	0.703	1.283
	u_{21}^{st}	3.452	1.503	2.141	3.564	1.517	2.217	3.606	1.515	2.246
	u_{31}^{st}	5.228	2.175	2.816	5.362	2.185	2.885	5.405	2.178	2.909
	u_{41}^{st}	6.496	2.638	3.274	6.638	2.644	3.339	6.679	2.633	3.358
	u_{51}^{st}	7.190	2.870	3.501	7.323	2.871	3.561	7.359	2.857	3.577
6	$u_1^{st} =$ u_{11}^{st}	1.394	0.704	1.080	1.454	0.721	1.141	1.479	0.726	1.169
	u_{21}^{st}	3.543	1.639	2.162	3.647	1.655	2.228	3.682	1.654	2.253
	u_{31}^{st}	5.623	2.470	3.008	5.748	2.480	3.068	5.781	2.472	3.084
	u_{41}^{st}	7.334	3.131	3.671	7.466	3.137	3.725	7.493	3.122	3.734
	u_{51}^{st}	8.530	3.578	4.114	8.660	3.579	4.163	8.681	3.560	4.168
	u_{61}^{st}	9.208	3.808	4.342	9.323	3.803	4.384	9.334	3.781	4.386
7	$u_1^{st} =$ u_{11}^{st}	1.646	0.825	1.264	1.622	0.813	1.252	1.743	0.850	1.367
	u_{21}^{st}	4.221	1.935	2.548	4.219	1.919	2.528	4.378	1.951	2.652
	u_{31}^{st}	6.779	2.959	3.594	6.811	2.934	3.563	6.976	2.959	3.679
	u_{41}^{st}	9.061	3.834	4.473	9.081	3.802	4.434	9.242	3.818	4.544
	u_{51}^{st}	10.85	4.513	5.152	10.87	4.476	5.108	11.02	4.485	5.209
	u_{61}^{st}	12.07	4.966	5.601	12.09	4.923	5.551	12.24	4.929	5.649
	u_{71}^{st}	12.76	5.197	5.831	12.76	5.148	5.775	12.90	5.150	5.868
8	$u_1^{st} =$ u_{11}^{st}	1.559	0.818	1.151	1.621	0.839	1.211	1.645	0.844	1.237
	u_{21}^{st}	4.176	2.008	2.500	4.287	2.030	2.570	4.322	2.029	2.592
	u_{31}^{st}	6.933	3.154	3.676	7.068	3.169	3.736	7.097	3.157	3.747
	u_{41}^{st}	9.487	4.179	4.709	9.630	4.185	4.761	9.650	4.163	4.762
	u_{51}^{st}	11.66	5.038	5.571	11.81	5.036	5.615	11.81	5.004	5.607
	u_{61}^{st}	13.36	5.697	6.229	13.50	5.689	6.267	13.50	5.652	6.252
	u_{71}^{st}	14.53	6.135	6.665	14.66	6.120	6.697	14.64	6.078	6.677
	u_{81}^{st}	15.21	6.367	6.897	15.32	6.346	6.921	15.29	6.300	6.897

4.2.3 Distribution of story shears

As a result of modal expansion of effective earthquake forces $m1$, modal static responses of story shears from force vector s_n are computed. It is evident that the direction of external forces s_n is controlled by the algebraic sign of the natural mode shapes of vibration, and thereby these forces for the fundamental mode act in the same horizontal direction. Essentially, since the fundamental mode dominates the modal response of the considered frames, the distribution of story shears over the height of the structures is obtained only for the fundamental mode. This distribution is observed to not depend strongly on bay numbers. Accordingly, presented in Fig. 5 are mean first-mode story shears normalized with respect to total seismic mass. Even though the slight differences at upper stories, infill walls affect story shears particularly at lower stories. Infilled frames exhibit relatively larger shear forces at their lower stories in comparison to bare frames. At first floor level of infilled frames, an increase of between 1.6 and 2.7% is observed in comparison to bare frames. The same trend is more specifically observed in case of soft story frames and when compared to those of infilled frames, an increase between 3 and 7% in first-story shear forces of soft story frames, in average, is calculated. The comparison of first-story shear forces of soft story frames with those of bare frames yields relatively larger values between 5 and 9.1%.

The ground-level values of Fig. 5, i.e. base shears normalized with respect to total seismic mass, are

Table 6 Comparison of fundamental mode displacements

Story	$(u_1^{st})_{infilled}/(u_1^{st})_{bare}$			$(u_1^{st})_{soft\ story}/(u_1^{st})_{infilled}$		
Level	Two-bay	Three-bay	Four-bay	Two-bay	Three-bay	Four-bay
1	0.37	0.36	0.35	2.45	2.60	2.68
2	0.35	0.34	0.33	1.87	1.95	2.00
3	0.34	0.33	0.32	1.69	1.76	1.80
1	0.43	0.42	0.41	2.00	2.10	2.16
2	0.43	0.39	0.38	1.59	1.64	1.67
3	0.39	0.38	0.37	1.42	1.46	1.49
4	0.38	0.37	0.36	1.37	1.41	1.43
1	0.47	0.46	0.46	1.72	1.79	1.82
2	0.44	0.43	0.42	1.42	1.46	1.48
3	0.42	0.41	0.40	1.29	1.32	1.34
4	0.41	0.40	0.39	1.24	1.26	1.28
5	0.40	0.39	0.39	1.22	1.24	1.25
1	0.51	0.50	0.49	1.53	1.58	1.61
2	0.46	0.45	0.45	1.32	1.35	1.36
3	0.44	0.43	0.43	1.22	1.24	1.25
4	0.43	0.42	0.42	1.17	1.19	1.20
5	0.42	0.41	0.41	1.15	1.16	1.17
6	0.41	0.41	0.41	1.14	1.15	1.16
1	0.50	0.50	0.49	1.53	1.54	1.61
2	0.46	0.45	0.45	1.32	1.32	1.36
3	0.44	0.43	0.42	1.21	1.21	1.24
4	0.42	0.42	0.41	1.17	1.17	1.19
5	0.42	0.41	0.41	1.14	1.14	1.16
6	0.41	0.41	0.40	1.13	1.13	1.15
7	0.41	0.40	0.40	1.12	1.12	1.14
1	0.52	0.52	0.51	1.41	1.44	1.47
2	0.48	0.47	0.47	1.25	1.27	1.28
3	0.45	0.45	0.44	1.17	1.18	1.19
4	0.44	0.43	0.43	1.13	1.14	1.14
5	0.43	0.43	0.42	1.11	1.11	1.12
6	0.43	0.42	0.42	1.09	1.10	1.11
7	0.42	0.42	0.42	1.09	1.09	1.10
8	0.42	0.41	0.41	1.08	1.09	1.09

participating mass ratios of the fundamental mode of the studied frames. Participating mass ratio of the fundamental mode increases in case of infilled frames, when compared to bare frames, and it attains higher values in case of soft story frames.

4.2.4 Lateral floor displacements

Listed in Table 5 are the fundamental mode static lateral displacements (u_{j1}^{st}) due to the effective earthquake forces in the fundamental mode s_1. The contribution of the fundamental mode to the force distribution $s=m1$ of the effective earthquake forces is the largest and the modal contributions to these forces decrease progressively in higher modes. As a consequence, as expected, the fundamental mode displacements dominate the total displacement distribution. Accordingly, the static floor displacements are given in particular for the fundamental mode in Table 5.

Values presented in Table 6 are the ratio of fundamental mode displacements of infilled frames to bare frames ($(u_1^{st})_{infilled}$ / $(u_1^{st})_{bare}$) and soft story frames to infilled frames ($(u_1^{st})_{soft\ story}$ / $(u_1^{st})_{infilled}$). The results show that infill walls significantly reduce static lateral displacements associated with the fundamental mode due to their high stiffness. The decreasing ratio, which is not very dependent to bay number, is found to be between 67% and 54% in average for 3 to 5 story frames whereas it is between 59% and 48% in average for 6 to 8 story frames, when the fundamental mode static lateral displacements of infilled frames are compared to those of bare frames. The decrease is greater at upper stories. It is quite apparent that infills are very influential on reducing lateral drifts. A more uniform lateral drift profile is observed for infilled frames in comparison to those for bare frames. This finding is consistent with Favvata *et al*. (2013) where it is found that the regular distribution of infills along the height of the structures resulted to smaller inter-story drifts in comparison to those of bare frames. A uniform lateral drift profile is also quite important since the internal forces in the structures are directly related to relative displacements, and further it is favorable to avoid second order effects.

In case of soft story irregularity, static lateral displacements at the first floor level are found to be closer to those of bare frames, whereas at the upper floor levels they are much closer to those of uniformly infilled frames, particularly when the number of story number is increased (Table 5). When the static lateral floor displacements of soft story frames are compared to those of infilled frames, a very significant increment, particularly at the first floor level, is observed. For example, 158%, 108% and 78% increment in average is calculated, respectively at the first floor levels of 3, 4 and 5 story frames. This ratio is relatively smaller at the first floor level of 6 to 8 story frames and calculated to be 58%, 56% and 44% in average, respectively at the first floor levels of 6, 7 and 8 story frames. A considerably high ratio of first-story static lateral displacement to second-story static lateral displacement is attained in case of soft story irregularity. Additionally, the increment ratio gradually decreases at upper stories. Soft story frames are found to exhibit the worst performance in terms of maximum requirements for inter-story drift at the first story (Favvata *et al*. 2003). Another interesting finding is that, when compared to uniformly infilled frames, static lateral displacements calculated at the floor levels of soft story frames are more dominant in low-rise frames.

5. Conclusions

The influence of infill walls on distribution of effective earthquake forces over the height of frames, and on some response quantities such as story shears, base shears and lateral floor displacements is investigated. The obtained results are mainly based on natural vibration properties of undamped 3 to 8 story bare, infilled and soft story frame structures, which enable a comparative assessment.

The variation in the spatial distribution of effective earthquake forces is particularly dominant in lower stories and they are found to increase when infill walls are considered. The earthquake forces at the first and the second floor levels of uniformly infilled frames increase with respect to story numbers. The increase in effective earthquake forces in uniformly infilled frames gradually decreases at upper stories. It is found that the variation in effective earthquake forces due to infill walls is insignificant in the last few stories. Furthermore, effective earthquake forces slightly decrease at the top story of infilled frames when compared to those of bare frames. A dramatic increase in effective earthquake forces at the first floor level is observed in case of soft story frames. It is observed that, infill walls and their distribution over the height of the structure also affect the higher modes of vibration and higher mode shapes of vibration do not remain unchanged in comparison to bare frames. Accordingly, the spatial distribution of effective earthquake forces is different for the higher modes in comparison to bare frames. On the other hand, the response contribution of higher modes is also generally insignificant both in case of uniformly infilled and soft story frames.

Base shear to seismic mass ratio are found to increase due to infill walls and this increase is much higher in case of soft story frames. Accordingly, it can be concluded that the potential seismic demand in terms of base shears increases due to infill walls and their distribution over the height of the structure. Both uniformly infilled and soft story frames exhibit relatively larger shear forces at their lower stories in comparison to bare frames. Infill walls significantly reduce static lateral floor displacements whereas the increase is greater at the first floor level in comparison to inter floor displacements. Although infill walls affect the spatial distribution of modal inertia forces, as well as of story and base shears, by contributing the elastic stiffness of structures, this variation is not very dependent to bay number of frames. It is observed that, frames with different bays exhibit nearly the same trend in variation of effective earthquake forces.

References

Akhoundi, F., Vasconcelos, G., Lourenço, P., Palha, C. and Silva, L. (2015), “In-plane and out-of plane experimental characterization of RC masonry infilled frames”, *Proceedings of the 6th International Conference on Mechanics and Materials in Design*, P. Delgada, Portugal, July.

Asteris, P.G. (2008), “Finite element micro-modeling of infilled frames”, *Electron. J. Struct. Eng.*, **8**, 1-11.

Asteris, P.G., Cavaleri, L., Di Trapani, F. and Tsaris, A.K. (2017), “Numerical modelling of out-of-plane response of infilled frames: State of the art and future challenges for the equivalent strut macromodels”, *Eng. Struct.*, **132**, 110-122. https://doi.org/10.1016/j.engstruct.2016.10.012.

ASCE/SEI 41-06 (2007), Seismic rehabilitation of existing buildings, American Society of Civil Engineers; Reston, Virginia, United States.

ASCE/SEI 41-13 (2014), Seismic evaluation and retrofit of existing buildings, American Society of Civil Engineers; Reston, Virginia, United States.

Blasi, G., De Luca, F. and Aiello, M.A. (2018), “Brittle failure in RC masonry infilled frames: The role of infill overstrength”, *Eng. Struct.*, **177**, 506-518. https://doi.org/10.1016/j.engstruct.2018.09.079.

Campione, G., Cavaleri, L., Macaluso, G., Amato, G. and Di Trapani, F. (2015), “Evaluation of infilled frames: an updated in-plane-stiffness macro-model considering the effects of vertical loads”, *Bull. Earthq. Eng.*, **13**(8), 2265-2281. https://doi.org/10.1007/s10518-014-9714-x.

Canbay, E., Ersoy, U. and Ozcebe, G. (2003), “Contribution of reinforced concrete infills to seismic behavior of structural systems”, *ACI Struct. J.*, **100**(5), 637-643.

Cavaleri, L. and Di Trapani, F. (2014), “Cyclic response of masonry infilled RC frames: Experimental results and simplified modeling”, *Soil Dyn. Earthq. Eng.*, **66**, 224-242. https://doi.org/10.1016/j.soildyn.2014.06.016.

Cavaleri, L. and Di Trapani, F. (2015), “Prediction of the additional shear action on frame members due to infills”, *Bull. Earthq. Eng.*, **13**(5), 1425-1454. https://doi.org/10.1007/s10518-014-9668-z.

Celarec, D. and Dolsek, M. (2013), “Practice-oriented probabilistic seismic performance assessment of infilled frames with consideration of shear failure of columns”, *Earthq. Eng. Struct. Dyn.*, **42**(9), 1339-1360. https://doi.org/10.1002/eqe.2275.

Celarec, D., Ricci, P. and Dolšek, M. (2012), “The sensitivity of seismic response parameters to the uncertain modelling variables of masonry-infilled reinforced concrete frames”, *Eng. Struct.*, **35**, 165-177. https://doi.org/10.1016/j.engstruct.2011.11.007.

Chopra, A.K. (2012), *Dynamics of Structures, Theory and*

Applications to Earthquake Engineering, Prentice Hall, Upper Saddle River, New Jersey, U.S.A.

Chrysostomou, C.Z. and Asteris, P.G. (2012), "On the in-plane properties and capacities of infilled frames", *Eng. Struct.*, **33**, 385-402. https://doi.org/10.1016/j.engstruct.2012.03.057.

Decanini, L., Mollaioli, F., Mura, A. and Saragoni, R. (2004), "Seismic performance of masonry infilled R/C frames", *13th World Conference on Earthquake Engineering*, Paper No. 165, Vancouver, B.C., Canada, August.

De Domenico, D., Falsone, G. and Laudani, R. (2018), "In-plane response of masonry infilled RC framed structures: A probabilistic macromodeling approach", *Struct. Eng. Mech.*, **68**(4), 423-442. https://doi.org/10.12989/sem.2018.68.4.423.

De Risi, M.T., Del Gaudio, C., Ricci, P. and Verderame, G.M. (2017), "Simplified numerical modelling for hollow clay-masonry infills in RC frames under in-plane seismic loads", *XVII ANIDIS Conference*, Pistoia, Italy, September.

Dolsek, M. and Fajfar, P. (2008), "The effect of masonry infills on the seismic response of a four-storey reinforced concrete frame – a deterministic assessment", *Eng. Struct.*, **30**(7), 1991-2001. https://doi.org/10.1016/j.engstruct.2008.01.001.

EC8 (2004), Eurocode 8: Design of structures for earthquake resistance-part 1: General rules, seismic actions and rules for buildings, European Committee for Standardization; Brussels, Belgium.

Emamia, S.M.M. and Mohammadi, M. (2016), "Influence of vertical load on in-plane behavior of masonry infilled steel frames", *Earthq. Struct.*, **11**(4), 609-627. https://doi.org/10.12989/eas.2016.11.4.609.

Favvata, M.J., Naoum, M.C. and Karayannis, C.G. (2013), "Limit states of RC structures with first floor irregularities", *Struct. Eng. Mech.*, **47**(6), 791-818. http://dx.doi.org/10.12989/sem.2013.47.6.791.

FEMA 356 (2000), Prestandard and commentary for the seismic rehabilitation of buildings, Federal Emergency Management Agency; Washington, D.C.

Fenerci, A., Binici, B., Ezzatfar, P., Canbay, E. and Ozcebe, G. (2016), "The effect of infill walls on the seismic behavior of boundary columns in RC frames", *Earthq. Struct.*, **10**(3), 539-562. https://doi.org/10.12989/eas.2016.10.3.539.

Fiore, A., Netti, A. and Monaco, P. (2012), "The influence of masonry infill on the seismic behaviour of RC frame buildings", *Eng. Struct.*, **44**, 133-145. https://doi.org/10.1016/j.engstruct.2012.05.023.

Furtado, A., Rodrigues, H. and Arêde, A. (2015), "Modelling of masonry infill walls participation in the seismic behaviour of RC buildings using OpenSees", *Int. J. Adv. Struct. Eng. (IJASE)*, **7**(2), 117-127. https://doi.org/10.1007/s40091-015-0086-5.

Furtado, A., Rodrigues, H., Arêde, A. and Varum, H. (2016), "Simplified macro-model for infill masonry walls considering the out-of-plane behavior", *Earthq. Eng. Struct. Dyn.*, **45**(4), 507-524. https://doi.org/10.1002/eqe.2663.

Furtado, A., Rodrigues, H., Arêde, A., Varum, H., Grubišić, M. and Šipoš, T.K. (2018), "Prediction of the earthquake response of a three-storey infilled RC structure", *Eng. Struct.*, **171**, 214-235. https://doi.org/10.1016/j.engstruct.2018.05.054.

Hak, S., Morandi, P., Magenes, G. and Sullivan, T.J. (2012), "Damage control for clay masonry infills in the design of RC frame structures", *J. Earthq. Eng.*, **16**(sup1), 1-35. https://doi.org/10.1080/13632469.2012.670575.

Haldar, P., Singh, Y. and Paul, D.K. (2013), "Identification of seismic failure modes of URM infilled RC frame buildings", *Eng. Fail. Anal.*, **33**, 97-118. https://doi.org/10.1016/j.engfailanal.2013.04.017.

Jiang, H., Liu, X. and Mao, J. (2015), "Full-scale experimental study on masonry infilled RC moment-resisting frames under cyclic loads", *Eng. Struct.*, **91**, 70-84. https://doi.org/10.1016/j.engstruct.2015.02.008.

Kakaletsis, D.J., David, K.N. and Karayannis, C.G. (2011), "Effectiveness of some conventional seismic retrofitting techniques for bare and infilled R/C frames", *Struct. Eng. Mech.*, **39**(4), 499-520. http://dx.doi.org/10.12989/sem.2011.39.4.499.

Karayannis, C.G., Favvata, M.J. and Kakaletsis, D.J. (2011), "Seismic behaviour of infilled and pilotis RC frame structures with beam–column joint degradation effect", *Eng. Struct.*, **33**(10), 2821-2831. https://doi.org/10.1016/j.engstruct.2011.06.006.

Kurt, E.G., Binici, B., Kurç, Ö., Canbay, E., Akpınar and Özcebe, G. (2011), "Seismic performance of a deficient reinforced concrete test frame with infill walls", *Earthq. Spectra*, **27**(3), 817-834. https://doi.org/10.1193/1.3609876.

Lima, C., De Stefano, G. and Martinelli, E. (2014), "Seismic response of masonry infilled RC frames: practice-oriented models and open issues", *Earthq. Struct.*, **6**(4), 409-436. https://doi.org/10.12989/eas.2014.6.4.409.

Lu, Y. (2002), "Comparative study of seismic behavior of multistory reinforced concrete framed structures", *J. Struct. Eng.*, **128**(2), 169-178. https://doi.org/10.1061/(ASCE)0733-9445(2002)128:2(169).

Lucchini, A., Mollaioli, F. and Bazzurro, P. (2014), "Floor response spectra for bare and infilled reinforced concrete frames", *J. Earthq. Eng.*, **18**(7), 1060-1082. https://doi.org/10.1080/13632469.2014.916633.

Manfredi, G., Ricci, P. and Verderame, G.M. (2012), "Influence of infill panels and their distribution on seismic behavior of existing reinforced concrete buildings", *Open Constr. Build. Technol. J.*, **6**, 236-253. http://doi.org/10.2174/1874836801206010236.

Manfredi, V. and Masi, A. (2014), "Combining in-plane and out-of-plane behaviour of masonry infills in the seismic analysis of RC buildings", *Earthq. Struct.*, **6**(5), 515-537. https://doi.org/10.12989/eas.2014.6.5.515.

Manos, G.C., Soulis, V.J. and Thauampteh, J. (2012), "The behavior of masonry assemblages and masonry-infilled R/C frames subjected to combined vertical and cyclic horizontal seismic-type loading", *Adv. Eng. Softw.*, **45**(1), 213-231. https://doi.org/10.1016/j.advengsoft.2011.10.017.

Mazza, F. (2015), "Comparative study of the seismic response of RC framed buildings retrofitted using modern techniques", *Earthq. Struct.*, **9**(1), 29-48. http://dx.doi.org/10.12989/eas.2015.9.1.029.

Morandi, P., Hak, S. and Magenes, G. (2014), "In-plane experimental response of strong masonry infills", *9th International Masonry Conference*, Guimarães, Portugal, July.

Muthukumar, S., Satyanarayanan, K.S. and Senthil, K. (2017), "Studies on two bay and three storey infilled frame with different interface materials: Experimental and finite element studies", *Struct. Eng. Mech.*, **64**(5), 543-555. https://doi.org/10.12989/sem.2017.64.5.543.

Onat, O., Correia, A.A., Lourenço, P.B. and Koçak, A. (2018), "Assessment of the combined in-plane and out-of-plane behavior of brick infill walls within reinforced concrete frames under seismic loading", *Earthq. Eng. Struct. Dyn.*, **47**(14), 2821-2839. https://doi.org/10.1002/eqe.3111.

Redmond, L., Ezzatfar, P., DesRoches, R., Stavridis, A., Ozcebe, G. and Kurc, O. (2016), "Finite element modeling of a reinforced concrete frame with masonry infill and mesh reinforced mortar subjected to earthquake loading", *Earthq. Spectra*, **32**(1), 393-414. https://doi.org/10.1193/081314EQS128M.

Repapis, C. and Zeris, C.A. (2019), "Seismic assessment of non-conforming infilled RC buildings using IDA procedures", *Front. Built Environ.*, **4**(88), 1-23. https://doi.org/10.3389/fbuil.2018.00088.

Ricci, P., Verderame, G.M. and Manfredi, G. (2011), "Analytical investigation of elastic period of infilled RC MRF buildings", *Eng. Struct.*, **33**(2), 308-319. https://doi.org/10.1016/j.engstruct.2010.10.009.

Rodrigues, H., Varum, H. and Costa, A. (2010), "Simplified macro-model for infill masonry panels", *J. Earthq. Eng.*, **14**(3), 390-416. https://doi.org/10.1080/13632460903086044.

SAP2000 Ultimate. (2018), Integrated Solution for Structural Analysis and Design, Version 20.2.0, Computers and Structures Inc. (CSI), Berkeley, California, USA.

Sassun, K., Sullivan, T.J., Morandi, P. and Cardone, D. (2016), "Characterising the in-plane seismic performance of infill masonry", *Bull. N.Z. Soc. Earthq. Eng.*, **49**(1), 100-117.

Šipoš, T.K., Sigmund, V. and Hadzima-Nyarko, M. (2013), "Earthquake performance of infilled frames using neural networks and experimental database", *Eng. Struct.*, **51**, 113-127. https://doi.org/10.1016/j.engstruct.2012.12.038.

Šiposa, T.K., Rodrigues, H. and Grubišića, M. (2018), "Simple design of masonry infilled reinforced concrete frames for earthquake resistance", *Eng. Struct.*, **171**, 961-981. https://doi.org/10.1016/j.engstruct.2018.02.072.

Stavridis, A. and Shing, P. B. (2010), "Finite-element modeling of nonlinear behavior of masonry-infilled RC frames", *J. Struct. Eng.*, **136**(3), 285-296. https://doi.org/10.1061/(ASCE)ST.1943-541X.116.

Su, R.K.L., Chandler, A.M., Sheikh, M.N. and Lam, N.T.K. (2005), "Influence of non-structural components on lateral stiffness of tall buildings", *Struct. Des. Tall Spec. Build.*, **14**(2). 143-164. https://doi.org/10.1002/tal.266.

Tabeshpour, M.R. and Arasteh, A.M. (2019), "A new method for infill equivalent strut width", *Struct. Eng. Mech.*, **69**(3), 257-268. https://doi.org/10.12989/sem.2019.69.3.257.

TSDC (2018). Turkish seismic design code, Ministry of Public Works and Settlement; Ankara, Turkey.

Tu, Y.H., Chuang, T.H., Liu, P.M. and Yang, Y.S. (2010), "Out-of-plane shaking table tests on unreinforced masonry panels in RC frames". *Eng. Struct.*, **32**(12), 3925-3935. https://doi.org/10.1016/j.engstruct.2010.08.030.

Uva, G., Porco, F. and Fiore, A. (2012), "Appraisal of masonry infill walls effect in the seismic response of RC framed buildings: A case study", *Eng. Struct.*, **34**, 514-526. https://doi.org/10.1016/j.engstruct.2011.08.043.

Uva, G., Raffaele, D., Porco, F. and Fiore, A. (2012), "On the role of equivalent strut models in the seismic assessment of infilled RC buildings", *Eng. Struct.*, **42**, 83-94. https://doi.org/10.1016/j.engstruct.2012.04.005.

Varela-Rivera, J.L., Navarrete-Macias, D., Fernandez-Baqueiro, L.E. and Moreno, E.I. (2011), "Out-of-plane behaviour of confined masonry walls", *Eng. Struct.*, **33**(5), 1734-1741. https://doi.org/10.1016/j.engstruct.2011.02.012.

Yekrangnia, M. and Mohammadi, M. (2017), "A new strut model for solid masonry infills in steel frames", *Eng. Struct.*, **135**, 222-235. https://doi.org/10.1016/j.engstruct.2016.10.048.

Zhai, C., Kong, J., Wang, X. and Chen, Z.Q. (2016), "Experimental and finite element analytical investigation of seismic behavior of full-scale masonry infilled RC frames", *J. Earthq. Eng.*, **20**(7), 1171-1198. https://doi.org/10.1080/13632469.2016.1138171.

Zhang, H., Kuang, J.S. and Yuen, T.Y.P. (2017), "Low-seismic damage strategies for infilled RC frames: shake-table tests", *Earthq. Eng. Struct. Dyn.*, **46**(4), 2419-2438. https://doi.org/10.1002/eqe.2911.

AT